



Amplification of waves from a rotating body

Marion Cromb¹, Graham M. Gibson¹, Ermes Toninelli¹, Miles J. Padgett¹✉, Ewan M. Wright² and Daniele Faccio^{1,2}✉

In 1971, Zel'dovich predicted that quantum fluctuations and classical waves reflected from a rotating absorbing cylinder will gain energy and be amplified. This concept, which is a key step towards the understanding that black holes may amplify quantum fluctuations, has not been verified experimentally owing to the challenging experimental requirement that the cylinder rotation rate must be larger than the incoming wave frequency. Here, we demonstrate experimentally that these conditions can be satisfied with acoustic waves. We show that low-frequency acoustic modes with orbital angular momentum are transmitted through an absorbing rotating disk and amplified by up to 30% or more when the disk rotation rate satisfies the Zel'dovich condition. These experiments address an outstanding problem in fundamental physics and have implications for future research into the extraction of energy from rotating systems.

In 1969, Roger Penrose proposed a method to extract the rotational energy of a rotating black hole, now known as Penrose superradiance¹. Penrose suggested that an advanced civilisation might one day be able to extract energy from a rotating black hole by lowering and then releasing a mass from a structure that is co-rotating with the black hole. Yakov Zel'dovich translated this idea of rotational superradiance from a rotating black hole to that of a rotating absorber such as a metallic cylinder, and showed it would amplify incident electromagnetic waves, even vacuum fluctuations, that had angular momentum^{2–4}. These ideas involving black holes and vacuum fluctuations converged in Stephen Hawking's 1974 prediction that non-rotating black holes will amplify quantum fluctuations, thus dissipating energy and eventually evaporating. Analogue laboratory experiments have been carried out that confirm these phenomena: Penrose superradiance, or superradiant scattering, in classical hydrodynamical vortices in the form of 'over-reflection'^{5,6} and classical forms of Hawking's predictions in flowing water⁷ and in optics^{8,9}, plus a quantum analogue in superfluids^{10–12}. However, Zel'dovich amplification in the form of amplification of waves from an absorbing cylinder has yet to be verified experimentally.

Zel'dovich found the general condition for amplification from an absorbing, rotating body:

$$\omega - \ell\Omega < 0 \quad (1)$$

where ω is the incident wave frequency, ℓ is the order of (what is referred to in the current literature as) the orbital angular momentum (OAM)^{13–15} and Ω is the rotation rate of the absorber. When this is satisfied, the absorption changes sign and the rotating medium acts as an amplifier. Outgoing waves then have an increased amplitude, therefore extracting energy from the rotational energy of the body in the spirit of Penrose's proposal.

To satisfy the condition in equation (1) with electromagnetic waves is extremely challenging. For $\ell = 1$ we would need rotation speeds Ω in the GHz to PHz region (microwave to optical frequencies), which is many orders of magnitude faster than the typical 100–1,000 Hz rotation speeds available for motor-driven mechanically rotating objects. The highest OAM reported to date in an experiment is of order $\ell \sim 10,000$ in the optical domain¹⁶, yet still leaves little hope of closing the rotation frequency gap to satisfy equation (1)^{17,18}.

However, recent work has shown that this condition and the observation of amplification is theoretically achievable with acoustic waves^{19–21}. The proposed interaction geometry requires sending an acoustic wave in transmission through a rotating absorbing disk. This provides a strong technical advantage compared to, for example, the sending of waves radially inwards towards the outer surface of a cylinder, as it allows us to use relatively low frequencies for both the waves and the disk rotation while keeping the dimensions sufficiently compact (the disk can be made very thin). An acoustic wave with OAM order ℓ will experience a rotational Doppler shift^{22,23} due to the disk rotation such that the wave frequency is shifted by a quantity $\omega - \ell\Omega$. This implies that the acoustic wave frequency will become negative when the Zel'dovich condition (equation (1)) is satisfied, which is precisely the prerequisite physical condition outlined by Zel'dovich in his original work. This condition was observed recently by ref. ²⁴ who measured the acoustic frequency with a rotating microphone. Although negative frequencies cannot be measured directly, the switch in sign of the acoustic wave frequency manifested itself as a switch in the sign of the wave orbital angular momentum, which was measured by tracking the phase difference between two closely spaced, co-rotating microphones.

In this work we demonstrate experimentally that Zel'dovich amplification is readily observable with acoustic waves with relatively low OAM ($\ell = 3, 4, 5$) and at low acoustic frequencies on the order of 60 Hz, which correspond to readily accessible rotation rates for the absorbing disk such that spurious signals (due to noise, for example) are also minimized. Our acoustic measurements are resolved as a spectrogram and analysed as a function of disk rotation frequency, showing an intensity gain of $\sim 30\%$ of acoustic energy over a range of orbital angular momenta. These measurements represent an important step forward in our understanding of Zel'dovich amplification, a fundamental wave–matter interaction that lies at the heart of a series of physical processes in condensed matter systems, superfluids and black holes.

Model

An acoustic conical wave carrying OAM ℓ is normally incident onto an absorbing material rotating at frequency Ω , and which is surrounded on both sides by non-rotating air. The acoustic wave

¹School of Physics and Astronomy, University of Glasgow, Glasgow, UK. ²Wyant College of Optical Sciences, University of Arizona, Tucson, AZ, USA.

✉e-mail: miles.padgett@glasgow.ac.uk; daniele.faccio@glasgow.ac.uk

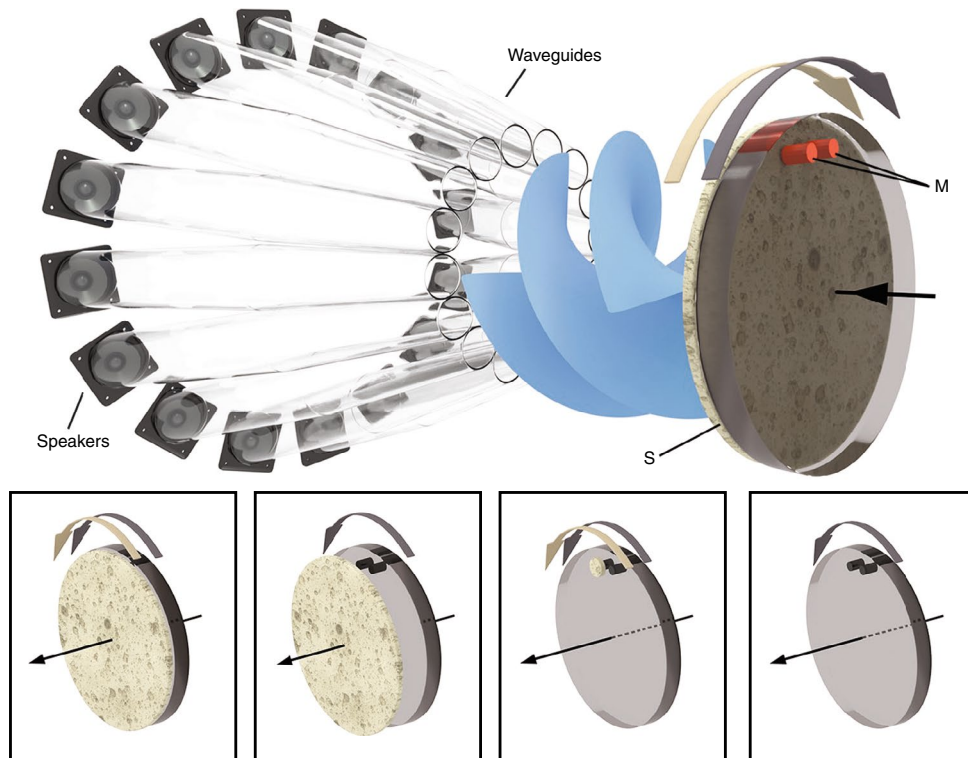


Fig. 1 | Schematic outline of experiment. Sixteen loudspeakers (Visaton, SC 8N) are arranged in a ring (diameter ≈ 0.47 m) to create an OAM acoustic field, channelled by acoustic waveguides to a smaller area (diameter ≈ 0.19 m) and incident on a rotating disk of sound-absorbing foam (S). The absorbing disk also carries two closely spaced (2 cm distance) microphones (M). The microphones transmit their data via Bluetooth (Avantree, Saturn Pro) for live data acquisition while in rotation. The set-up is adapted from that used by ref. ²⁴. Insets indicate the various configurations used in the experiments for the rotating disk and absorbing foam: left inset, the supporting disk with microphones and absorber are co-rotating; centre left inset, the absorber is detached and remains static, while microphones rotate; centre right inset, the absorber is placed in front of only one of the two microphones; right inset, the absorber is completely removed, and microphones rotate.

equation for density variations $\tilde{\rho}$ in a frame rotating with the medium is²⁵:

$$\frac{\partial^2 \tilde{\rho}}{\partial t^2} - \Gamma' \nabla^2 \frac{\partial \tilde{\rho}}{\partial t} - v^2 \nabla^2 \tilde{\rho} = 0 \quad (2)$$

where v is the sound velocity and Γ' the damping parameter. A similar wave equation applies in the surrounding air with sound velocity v_0 and $\Gamma' = 0$.

Under the condition that the medium length L is much less than the acoustic wavelength, the transmission of the beam incident from air onto the rotating medium may be solved by treating the effects of the medium absorption term in equation (2) within the first Born approximation. The details of this model have been worked out previously (supplementary material in ref. ¹⁹) and lead to the following expression for the acoustic beam transmittance:

$$T = \left[1 - \frac{L\omega^2}{k_z v^4} \Gamma'(\omega - \ell\Omega) \right] C(\omega) \quad (3)$$

where $k_z = (\omega/v) \cos \theta$ is the longitudinal component of the sound wavevector and can be controlled through the conical beam focusing angle, θ . We note that it is the term $(\omega - \ell\Omega)$ in the transmittance that can change the sign of the absorption and lead to gain in agreement with the Zel'dovich condition in equation (1).

Equation (3) also includes the frequency response of the microphones, $C(\omega)$. Standard microphones exhibit a roll-off in sensitivity starting below ~ 100 Hz. We model this response with a function $C(\omega) = 1 - \exp[-(\omega - \ell\Omega)^2/\sigma^2]$, where σ determines the rate at

which the sensitivity drops as a function of frequency. However, the precise form of this function is not critical to our main conclusions, as the experiments described below compare the results from two microphones with the same frequency response.

Experiments

We generate an acoustic wave with orbital angular momentum using a ring of speakers and tubes that guide the sound directly onto the rotating disk, as shown in Fig. 1. The ring of 16 loudspeakers are all driven at the same frequency ($\omega = 60$ Hz), each with a specific phase delay in order to approximate a helical phase front, generating a beam carrying OAM²⁴. Depending on the phase delay between adjacent speakers, different OAM states can be produced. For example, a phase delay of $\pi/2$ radians between adjacent speakers creates an OAM beam of topological charge $\ell = 4$.

A motor (RS Components, 536-6046) is used to rotate the disk fitted with two closely spaced microphones. Sound-absorbing material can be placed in front of both or one of the microphones, or it can be removed (as shown in Fig. 1). Test measurements are taken with the two microphones under experimental conditions to ensure that they exhibit the same acoustic response, with and without the absorbing material placed in front of them (see Methods). The data from the microphones are communicated via Bluetooth to a computer.

Figure 2 shows an example of a measured spectrogram. The acoustic frequency is set to 60 Hz on all of the speakers and phase delays are set to generate waves with $\ell = 4$, although other ℓ modes are expected to be generated also as a result of imperfections in speaker uniformity and the limited number of speakers used²⁴.

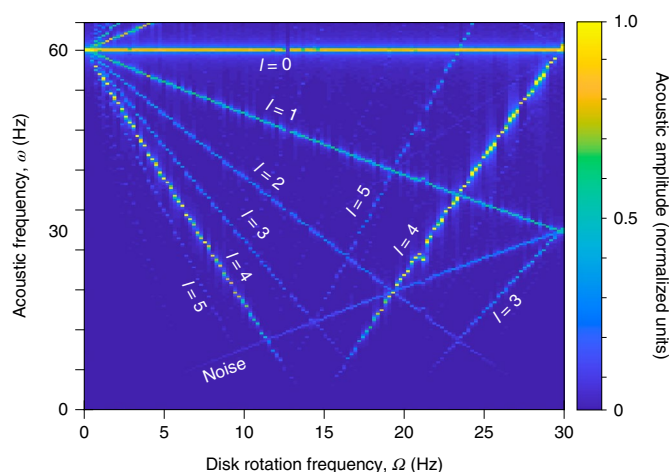


Fig. 2 | Spectrally resolved acoustic measurements. An example of a measured spectrogram showing the measured acoustic frequency (ω) spectrum in the rotating frame for increasing rotation frequencies (Ω). The OAM beam is generated in the laboratory frame at 60 Hz at a constant volume of -90 dB at the output of the waveguides, with the speaker output phases optimized for the $\ell = 4$ mode. For each value of Ω , the data show an independent spectrum, obtained from the Fourier transform of the measured signal from one of the two microphones on the rotating disk. The data clearly show the input 60 Hz signal split into multiple components, corresponding to the various OAM modes (indicated in the graph), as a result of a rotational Doppler shift, $\omega - \ell\Omega$, that leads to linearly varying frequency as a function of Ω for each ℓ mode. The microphone response decreases for decreasing measured ω and is zero (that is, below the noise level) below 4 Hz. Supplementary Video 1 shows an animation with the overlaid acoustic signal that is recorded with increasing Ω .

Therefore, the Zel'dovich condition and inversion from absorption to gain is expected for a disk rotation of 15 Hz. The disk is rotated in the 0 to 30 Hz range, which also corresponds to the linear response range of our motor (that is, the linear increase of rotation speed with driving voltage). The spectrogram exhibits a series of features: as the disk rotation rate increases, the input 60 Hz frequency splits into a series of signals, depending on the OAM value ℓ , with a clear signal measured for $\ell = 0 - 5$ (as labelled in the figure). We can also clearly see an additional signal that is due to the noise generated by the rotation and therefore appears at the same frequency as the rotation rate.

All of the observed OAM modes shift in frequency due to the rotational Doppler shift ($\Delta\omega = -\ell\Omega$), and after the labelled OAM modes have gone through zero frequency they satisfy their Zel'dovich condition. Beyond zero, the rotational Doppler shift formula predicts negative frequencies, which results in an inversion of the sign of ℓ (positively sloped traces in the spectrogram) when measured in the rotating frame²⁴. To verify the presence of gain in this Zel'dovich regime, we extract the amplitude for each ℓ value from the spectrograms.

Results

Figure 3 shows the effect of rotation on transmitted acoustic signal for the $\ell = 4$ mode as the disk rotation rate is increased from 0 to 30 Hz. The two curves indicate two different cases: the absorbing disk is co-rotating with the microphones, and the absorbing disk is slightly detached from the motor mount so that the microphones rotate while the disk remains static. As the rotation speed is increased, the modes are Doppler shifted and the measured signal from both microphones decreases due to the lower microphone response at lower acoustic frequencies. As the mode is Doppler

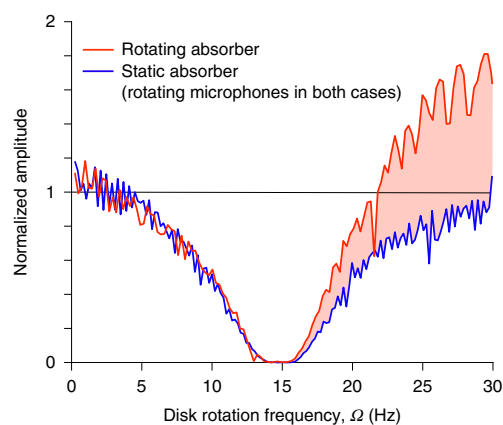


Fig. 3 | The effect of rotation. A measurement of the acoustic amplitude for $\ell = 4$ for the case of a rotating absorber (red curve) and for the case in which the absorber is detached from the rotating disk holding the microphones, and hence is static (blue curve). The rotating absorber case shows a clear increase of the transmitted acoustic amplitude above the Zel'dovich condition ($\omega - \ell\Omega < 0$ is satisfied for this case when $\Omega > 15$ Hz).

shifted through zero frequency (at $\Omega = 15$ Hz), the measured acoustic frequency increases again and the transmitted signal increases. In the non-rotating case, no increase is observed in the transmitted signal for the same rotational Doppler shift (that is, for symmetric points around $\Omega = 15$ Hz). Conversely, when the absorber is in rotation and there are no other changes to the experiment, we observe a clear increase in the transmitted signal at high rotation rates that satisfy the Zel'dovich condition.

Figure 4 shows evidence of absolute gain in the acoustic signal: the transmitted energy is larger than the incident energy. One microphone (microphone 1) in the rotating frame has absorbing foam in front of it, while the microphone next to it (microphone 2) does not. We observe that at low rotation speeds (2–5 Hz), the transmitted signal to microphone 1 is lower than that to microphone 2, as the incident signal has been absorbed by the foam. Conversely, rotation rates of greater than $\Omega = 15$ Hz, which satisfy the Zel'dovich condition, lead to a clear increase in the transmission signal compared to the non-absorbing case. The amplification is such that the signal transmitted through the absorber above $\Omega = 25$ Hz is greater by about 30% than the signal at the slowest rotation speeds that did not pass through the absorber. This indicates absolute gain: we measure more sound with the rotating absorber than without it.

The thick solid curves in Fig. 4 show the theoretical predictions from equation (3). First we fit equation (3) to the data from microphone 2 that has no absorber present ($\Gamma' = 0$), thus obtaining the shape of $C(\omega)$, the frequency response of the microphones. This determines the frequency sensitivity parameter, $\sigma = 22$ Hz. Then we refer to the data from microphone 1 and use the low rotation frequency (2–5 Hz) data to determine the value of the dissipation parameter, $\Gamma' = 8 \times 10^4 \text{ m}^2 \text{ s}^{-1}$. We notice that the same theoretical curve provides a quantitatively accurate prediction of the full behaviour for all Ω , including the 30% gain measured at high rotation frequencies, thus further corroborating the interpretation that the gain originates from the Zel'dovich effect.

Further analysis (Fig. 5) of multiple OAM modes transmitted through the rotating absorber reveals amplification for all of the OAM modes analysed that satisfy the Zel'dovich condition, not just the strongest $\ell = 4$ mode. At a more detailed level, if we consider a fixed Doppler-shifted frequency (for example, $\omega - \ell\Omega = -30$ Hz for all ℓ , corresponding to $\Omega = 30, 22.5$ and 18 Hz for $\ell = 3, 4$ and 5, respectively), we note that all curves within the experimental

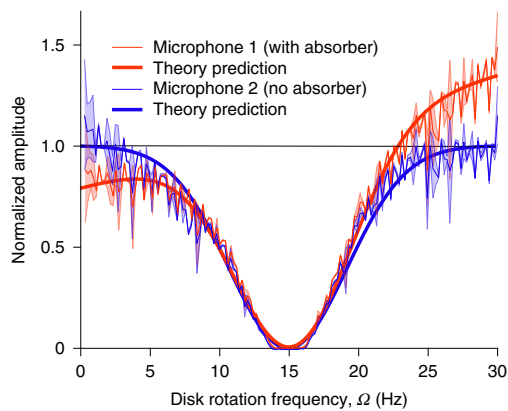


Fig. 4 | Evidence of absolute gain. The measured acoustic amplitude with $\ell = 4$ and with the absorber placed on one of the microphones (red curve) but not on the other (blue curve) shows clear differences in the signals. For rotation rates of $\Omega < 15$ Hz (such that $\omega - \ell\Omega > 0$), absorption is observed, in particular at the lowest frequencies. Conversely, at the highest frequencies (where $\omega - \ell\Omega < 0$), a clear gain in the transmitted signal is observed. The ~ 1.3 times higher signal at $\Omega \sim 30$ Hz compared to $\Omega \sim 0$ Hz highlights the presence of absolute gain of the acoustic signal. Theoretical predictions from equation (3) are shown with the damping parameter $\Gamma' = 0 \text{ m}^2 \text{ s}^{-1}$ (no absorber, thick blue curve) and $\Gamma' = 8 \times 10^4 \text{ m}^2 \text{ s}^{-1}$ (thick red curve). The shaded areas show the standard deviation of the measured signals across seven sets of data (2 s of acquisition each).

error show the same gain of $\sim 10\%$ (Fig. 5). If instead we consider a fixed disk rotation frequency (for example, $\Omega = 30$ Hz), we see that the gain (the transmitted acoustic energy) increases linearly with ℓ . Both of these observations are in agreement with the theoretical prediction (equation (3)).

Conclusions

Amplification of waves from a rotating absorber as predicted by Zel'dovich is a foundational prediction in fundamental physics that lies somewhere between the proposition by Penrose that energy can be extracted from rotating black holes and Hawking's prediction that static black holes will evaporate as a result of the interaction with quantum vacuum. Zel'dovich's original model indeed referred to amplification of vacuum modes from a rotating metallic cylinder but also was extended to include the amplification of classical waves. Although amplification of waves due to a rotating absorber is very hard to verify with optical or electromagnetic waves, direct measurements of it are possible using acoustic waves. A key step in achieving this result is the use of a geometry in which the waves are transmitted through a thin absorbing cylinder^{19–21} rather than in reflection from an extended cylinder. This relaxes the experimental constraints and limitations that arise in the original proposal from the requirement that the cylinder length is larger than the wavelength to ensure interaction and reflection of the incident waves. For example, this would have required a cylinder with a length of several metres for the conditions used here, which would have been very challenging to rotate at 30 Hz.

Similar concepts could in principle be extended to electromagnetic waves¹⁸, thus possibly extending our results to the amplification of electromagnetic modes from the quantum vacuum.

Online content

Any methods, additional references, Nature Research reporting summaries, source data, extended data, supplementary information, acknowledgements, peer review information; details of author contributions and competing interests; and statements of

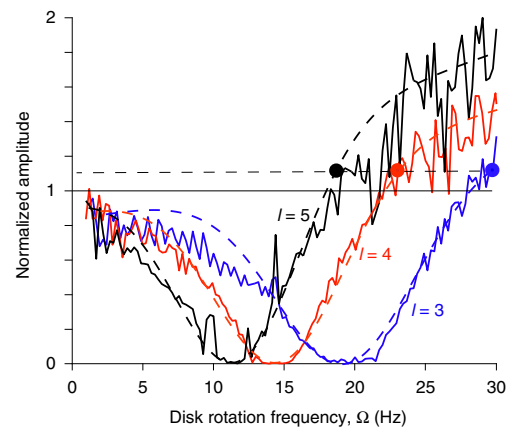


Fig. 5 | Comparison of different OAM beams. The spectrograms show signals for a range of ℓ that can also be analysed and compared. For all ℓ that pass through the Zel'dovich condition we see evidence of transmittance greater than 1 as a result of rotation. When the transmission values for the same rotational Doppler-shifted frequency (~ 30 Hz, corresponding to $\Omega = 30, 22.5$ and 18 Hz (filled circles) for $\ell = 3, 4$ and 5 , respectively) are compared, the gain in transmittance seems to be constant at ~ 1.1 (horizontal dashed line) for all ℓ , within experimental error. Furthermore, the amplification increases linearly with ℓ for a fixed Ω (compare the values for the different orders at $\Omega = 30$ Hz, for example). Both observations confirm the predictions of equation (3). Theoretical fits from equation (3) with no varying parameters (other than ℓ) are shown as dashed curves.

data and code availability are available at <https://doi.org/10.1038/s41567-020-0944-3>.

Received: 13 April 2020; Accepted: 20 May 2020;

Published online: 22 June 2020

References

- Penrose, R. Gravitational collapse: the role of general relativity. *Riv. Nuovo Cim. Num. Spec.* **1**, 257–276 (1969).
- Zel'dovich, Ya. B. Generation of waves by a rotating body. *JETP Lett.* **14**, 180–181 (1971).
- Zel'dovich, Ya. B. Amplification of cylindrical electromagnetic waves reflected from a rotating body. *J. Exp. Theor. Phys.* **35**, 1085–1087 (1972).
- Zel'dovich, Ya. B., Rozhanskii, L. V. & Starobinski, A. A. Rotating bodies and electrodynamics in a rotating coordinate system. *Radiophys. Quantum Electron.* **29**, 761–768 (1986).
- Acheson, D. J. On over-reflexion. *J. Fluid Mech.* **77**, 433–472 (1976).
- Torres, T. et al. Rotational superradiant scattering in a vortex flow. *Nat. Phys.* **13**, 833–836 (2017).
- Weinfurter, S., Tedford, E. W., Penrice, M. C. J., Unruh, W. G. & Lawrence, G. A. Measurement of stimulated Hawking emission in an analogue system. *Phys. Rev. Lett.* **106**, 021302 (2011).
- Belgiorno, F. et al. Hawking radiation from ultrashort laser pulse filaments. *Phys. Rev. Lett.* **105**, 203901 (2010).
- Drori, J., Rosenberg, Y., Bermudez, D., Silberberg, Y. & Leonhardt, U. Observation of stimulated Hawking radiation in an optical analogue. *Phys. Rev. Lett.* **122**, 010404 (2019).
- Steinhauer, J. Observation of self-amplifying Hawking radiation in an analogue black-hole laser. *Nat. Phys.* **10**, 864–869 (2014).
- Steinhauer, J. Observation of quantum Hawking radiation and its entanglement in an analogue black hole. *Nat. Phys.* **12**, 959–965 (2016).
- Muñoz de Nova, J. R., Golubkov, K., Kolobov, V. I. & Steinhauer, J. Observation of thermal Hawking radiation and its temperature in an analogue black hole. *Nature* **569**, 688–691 (2019).
- Allen, L., Beijersbergen, M. W., Spreeuw, R. J. C. & Woerdman, J. P. Orbital angular momentum of light and the transformation of Laguerre-Gaussian laser modes. *Phys. Rev. A* **45**, 8185–8189 (1992).
- Andrews, D. & Babiker, M. *The Angular Momentum of Light* (Cambridge Univ. Press, 2012).

15. Padgett, M., Courty, J. & Allen, L. Light's orbital angular momentum. *Phys. Today* **57**, 35–40 (2004).
16. Fickler, R., Campbell, G., Buchler, B., Lam, P. K. & Zeilinger, A. Quantum entanglement of angular momentum states with quantum numbers up to 10,010. *Proc. Natl Acad. Sci. USA* **113**, 13642–13647 (2016).
17. Faccio, D. & Wright, E. M. Nonlinear Zel'dovich effect: parametric amplification from medium rotation. *Phys. Rev. Lett.* **118**, 093901 (2017).
18. Gooding, C., Weinfurter, S. & Unruh, W. G. Reinventing the Zel'dovich wheel. Preprint at <https://arxiv.org/abs/1907.08688> (2019).
19. Faccio, D. & Wright, E. M. Superradiant amplification of acoustic beams via medium rotation. *Phys. Rev. Lett.* **123**, 044301 (2019).
20. Gooding, C., Weinfurter, S. & Unruh, W. G. Superradiant scattering of orbital angular momentum beams. Preprint at <https://arxiv.org/abs/1809.08235> (2020).
21. Gooding, C. Dynamics landscape for acoustic superradiance. Preprint at <https://arxiv.org/abs/2002.05605> (2020).
22. Courty, J., Robertson, D. A., Dholakia, K., Allen, L. & Padgett, M. J. Rotational frequency shift of a light beam. *Phys. Rev. Lett.* **81**, 4828–4830 (1998).
23. Bialynicki-Birula, I. & Bialynicka-Birula, Z. Rotational frequency shift. *Phys. Rev. Lett.* **78**, 2539–2542 (1997).
24. Gibson, G. M. et al. Reversal of orbital angular momentum arising from an extreme Doppler shift. *Proc. Natl Acad. Sci. USA* **115**, 3800–3803 (2018).
25. Boyd, R. *Nonlinear Optics* 3rd edn (Academic Press, 2008).

Publisher's note Springer Nature remains neutral with regard to jurisdictional claims in published maps and institutional affiliations.

© The Author(s), under exclusive licence to Springer Nature Limited 2020

Methods

The rotation speed of the absorber was increased in steps of (approximately) 0.2 Hz. Various forms of sound-absorbing foam were tested with varying yet similar porosity (for example, cellular ethylene propylene diene monomer, soundproofing rubber, RS Components, 5% absorption at 60 Hz). All cases showed similar results, consistent with our expectation that details in the medium 4–5 orders of magnitude smaller than the sound wavelength will not greatly influence the dynamics.

A photograph of the sound-absorber interaction region is shown in the Extended Data Fig. 1. The acoustic waveguides conduct the sound towards and directly on to the rotating absorber. The absorbing foam is held in place with a support structure, which is made of a plastic disk with no air gaps or possibility for sound to reach the microphones (5 mm diameter, embedded in the supporting plastic disk) without passing through the foam. This set-up ensures that all sound reaches the microphones only through the foam.

For each rotation speed, sound was recorded for short time intervals, such as 2–3 s. Then the microphone signal was Fourier transformed (and averaged over two to three separate measurements) to decompose the signal into its frequency spectrum. The frequency spectrum for each rotation speed was then used to create a single matrix of the full spectrogram (as in Fig. 2). In MATLAB R2018b the ‘tfridge’ range of functions was used to extract the signal amplitude (in arbitrary units) along each OAM mode in this spectrogram. The highest neighbouring frequency bin for each rotation speed was added to the signal to reduce noise from the discretisation of the Fourier-transformed data.

We also verified that the two microphones in our set-up were calibrated so as to provide the same response for the same incident signal, for all rotation speeds (see Extended Data Figs. 2 and 3).

Data availability

Source data are provided with this paper. All other data used to make the figures in this paper and other findings of this study are available from the corresponding author upon reasonable request.

Acknowledgements

This work was supported by the UK EPSRC (grant no. EP/P006078/2) and the Horizon 2020 research and innovation programme of the European Union (grant agreement no. 820392).

Author contributions

M.C. performed the measurements and data analysis. G.M.G., E.T. and M.C. built the experiment. E.M.W., D.F. and M.J.P. conceived the experiment and theory. All authors contributed to the manuscript.

Competing interests

The authors declare no competing interests.

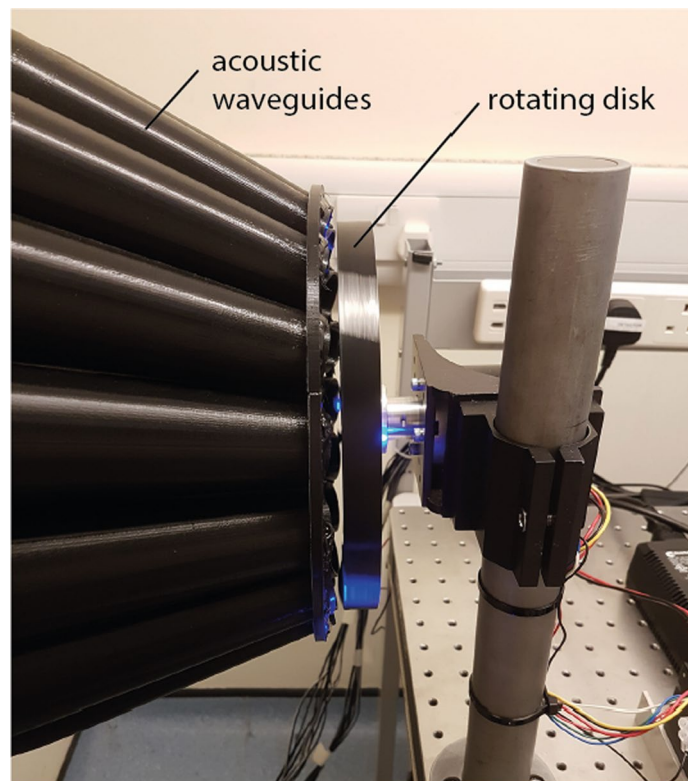
Additional information

Extended data is available for this paper at <https://doi.org/10.1038/s41567-020-0944-3>.

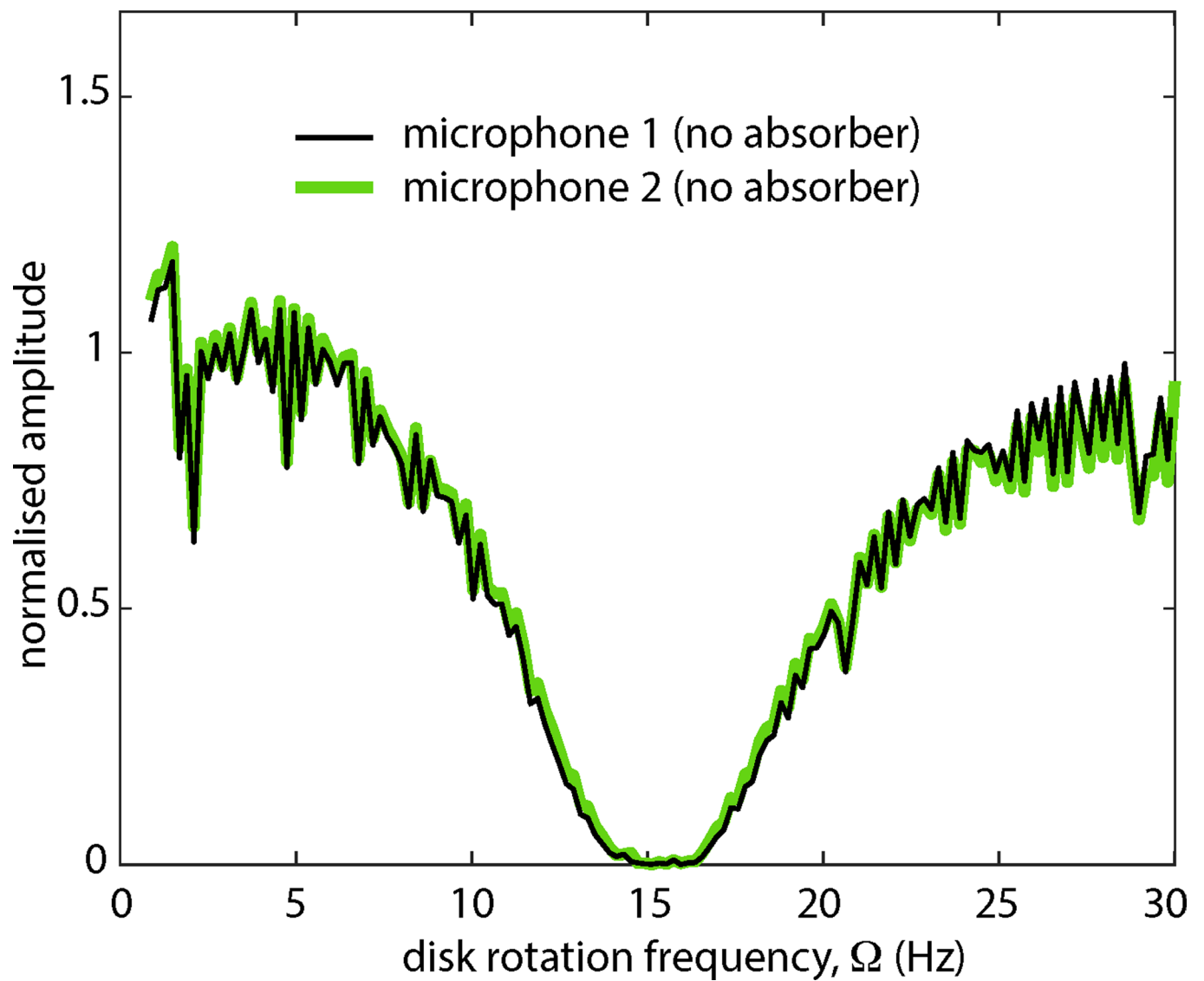
Supplementary information is available for this paper at <https://doi.org/10.1038/s41567-020-0944-3>.

Correspondence and requests for materials should be addressed to M.J.P. or D.F.

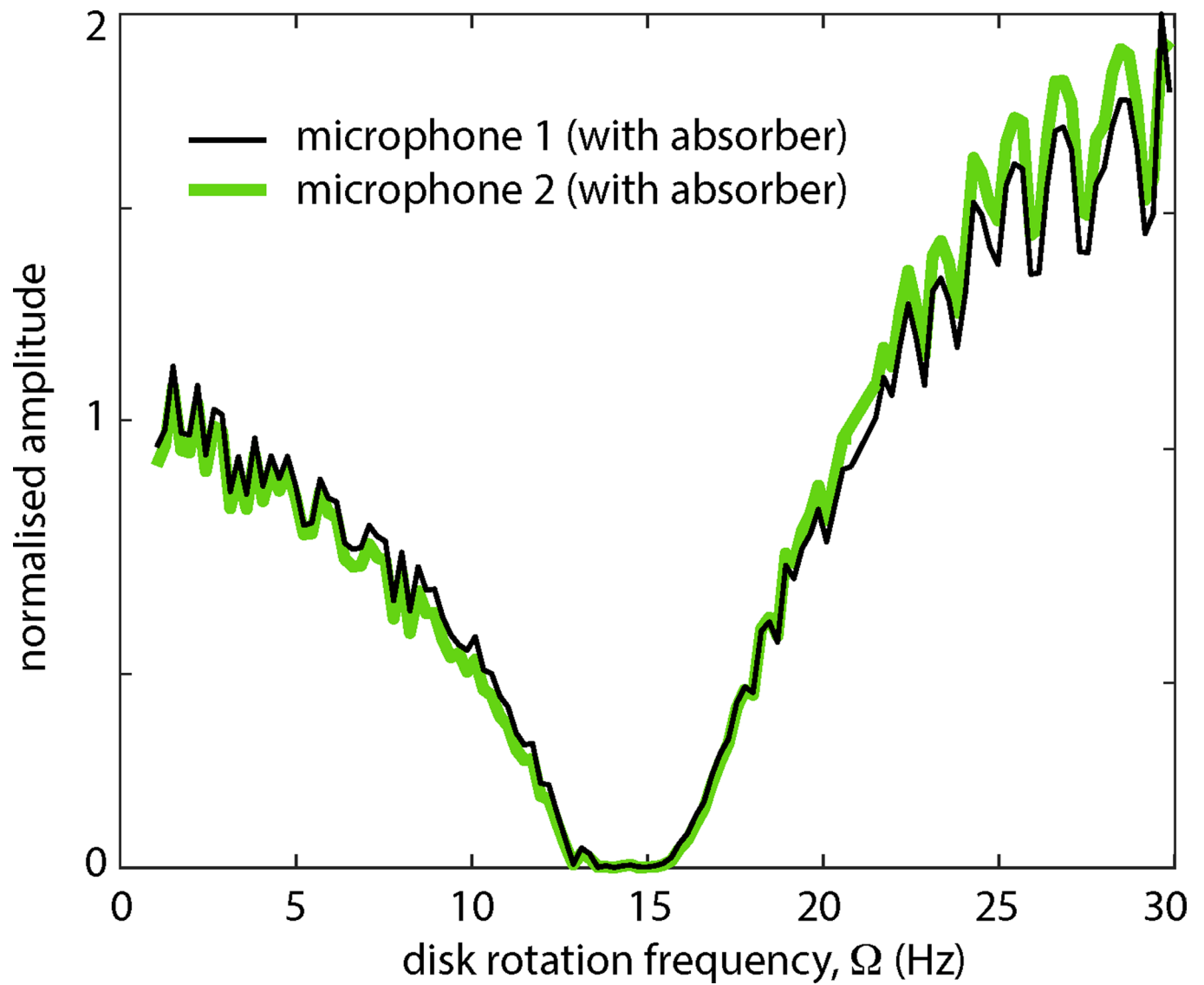
Reprints and permissions information is available at www.nature.com/reprints.



Extended Data Fig. 1 | Photograph of set-up. Photograph of the set-up showing the detail of the interaction region where the acoustic waveguides conduct the sound directly on to the absorber, supported by a plastic disk.



Extended Data Fig. 2 | Microphone response (with no absorber). Microphone calibration: measurements of response when both microphones have no absorber placed in front of them, showing that the microphones are both calibrated and measure the same signal, as desired.



Extended Data Fig. 3 | Microphone response (with absorber). Microphone calibration: measurements of response when both microphones have absorbers placed in front of them, showing that the microphones are both calibrated and measure the same signal, as desired.